Measurement of Multiscale Thermal Transport Phenomena in Li-Ion Cells: A Review

Krishna Shah[1]

Mechanical and Aerospace
Engineering Department,
University of Texas at Arlington,
Arlington, TX 76019

Vivek Vishwakarma[1]

Mechanical and Aerospace
Engineering Department,
University of Texas at Arlington,
Arlington, TX 76019

Ankur Jain[2]

Mechanical and Aerospace
Engineering Department,
University of Texas at Arlington,
500 West First Street, Rm 211,
Arlington, TX 76019
e-mail: jaina@uta.edu

The performance, safety, and reliability of electrochemical energy storage and conversion systems based on Li-ion cells depend critically on the nature of heat transfer in Li-ion cells, which occurs over multiple length scales, ranging from thin material layers all the way to large battery packs. Thermal phenomena in Li-ion cells are also closely coupled with other transport phenomena such as ionic and charge transport, making this a challenging, multidisciplinary problem. This review paper presents a critical analysis of recent research literature related to experimental measurement of multiscale thermal transport in Li-ion cells. Recent research on several topics related to thermal transport is summarized, including temperature and thermal property measurements, heat generation measurements, thermal management, and thermal runaway measurements on Li-ion materials, cells, and battery packs. Key measurement techniques and challenges in each of these fields are discussed. Critical directions for future research in these fields are identified. [DOI: 10.1115/1.4034413]

Keywords: Li-ion cells, multiscale thermal transport, thermal properties, thermal runaway, heat generation, temperature measurement

1 Introduction

Li-ion cells are used for energy conversion and storage in a wide variety of applications, including consumer electronics, electric vehicles, aerospace systems, etc. [1–3]. Energy storage in hybrid and electric vehicles tremendously improves fuel efficiency, while also offering reduced emissions and other environmental benefits [4]. In other applications, Li-ion cells enable energy storage and conversion at very high density and rates compared to competing technologies [1,5]. The capability of high-efficiency energy storage facilitates the harnessing of renewable energy sources such as wind energy and solar energy [6], where energy storage is critical. Among several competing energy storage mechanisms, electrochemical energy storage in Li-ion cells offers several advantages in terms of energy density, power, etc. [3,7], which has spurred significant amount of research in this technology.

From a scientific perspective, a Li-ion cell involves several multidisciplinary and multiscale processes that are closely coupled with each other [7–9], as shown in Fig. 1. One such example is the coupling between thermal transport and electrochemical processes. Electrochemical reactions in a Li-ion cell generate heat, which influences the temperature distribution. The temperature distribution in turn governs the electrochemical reaction kinetics, ionic charge transport, and crystalline phase equilibria of the electrodes. The dynamics of these phenomena are strongly coupled. For example, in addition to the thermal properties of the cell, temperature rise during discharge also depends on electrochemical properties such as equivalent series resistance (ESR). At the same time, electrochemical processes in the cell are themselves strong functions of temperature. As a result, thermal transport plays a key role in determining the electrochemical performance of the cell, particularly for high-rate processes.

As shown in Fig. 1, the electrical, electrochemical, and thermal phenomena occurring in a Li-ion cell interact with each other through well-known processes, such as species diffusion, charge transport, chemical kinetics, thermal transport, etc. These processes are governed by physical laws involving multiple transport properties such as thermal conductivity, mass diffusivity, reaction rates, etc. Due to the heterogeneous nature of materials inside a Li-ion cell, these properties are often not well known in advance. In addition, these properties are often strong functions of temperature and electrochemical state of the cell, with significant spatial variation within the cell volume as well.

Further, these coupled phenomena occur over multiple length scales [8–10], as shown in Fig. 2. At the molecular level, pertinent processes include Li-ion intercalation in the electrode materials, species transport, etc. [7,11–13]. Electrode layers, typically 5–50 μm thick, and a porous separator, are rolled or folded into cells [14,15], which are then integrated in a battery pack [16] (Fig. 4). The morphology and chemical composition of layers, overall packaging within a cell, and the arrangement of cells in a battery pack all influence the nature of physical processes that determine performance, safety, and reliability.

Heat generation is an inevitable effect of energy conversion and storage processes in a Li-ion cell. In order to avoid several well-known performance and safety problems at high temperatures [17–19], heat generated throughout the volume of the cell due to ionic resistance and exothermic reactions [20–23] must be removed through the various materials and within the cell to its outer surface, and from there to the ambient mostly through
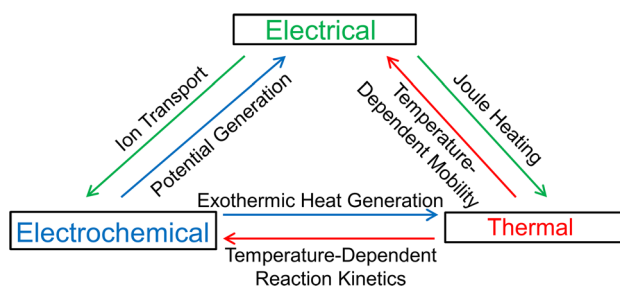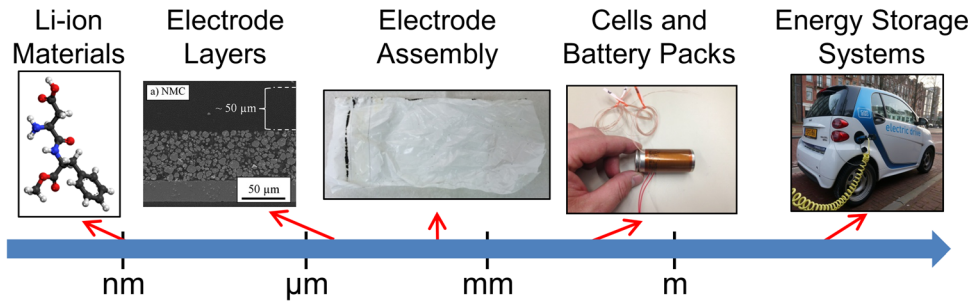

Fig. 1 Schematic showing three significant categories of physical processes and the nature of their interactions in a Li-ion cell

---

Fig. 2 Schematic showing the multiscale nature of Li-ion based electrochemical energy storage and conversion

thermal conduction and convection [24–26], but also possibly through radiative thermal transport. Figure 3 shows a schematic of key thermal resistances in a Li-ion cell—thermal conduction within the cell and convection on the outside surface. The thermal conduction resistance itself can be broken down into contributions from various material and interfacial thermal resistances in the thermal unit cell as shown in Fig. 3. While heat generation is closely coupled with electrochemical state of the cell and the nature of electrochemical reactions in the cell, the heat transfer is governed by the nature of materials and interfaces within the cell, as well as ambient thermal conditions around the cell. These processes, their interactions with each other, as well as with other physical phenomena combine to determine the thermal state of the cell. While low-temperature operation of Li-ion cells has attracted some research due to potential problems in automotive applications [27,28], much more work has focused on understanding thermal transport in high-temperature situations where thermal runaway poses a significant safety risk. The analysis and prevention of thermal runaway is a complex, coupled problem requiring an understanding of electrochemistry as well as thermal transport.

Thermal management of the battery pack is critically needed in both nominal and abuse conditions. Several aspects of a Li-ion cell make the overall thermal transport process interesting and challenging to model and measure. These include materials with uncharacterized thermal properties, unknown nature of thermal transport at material interfaces, coupled nature of thermal transport with electrochemistry, thermal conduction anisotropy, nonlinear behavior at high temperatures, etc. Despite these challenges, there are strong incentives for studying and optimizing thermal transport in a Li-ion cell. Improved thermal transport will help not only safety but also electrochemical performance. As a general example, if the temperature rise in a Li-ion cell due to a given heat generation rate can be reduced through effective thermal management, it would enable operation of the cell at greater discharge rates, thereby improving pack-level performance, weight, etc.

This paper reviews pertinent recent literature on various aspects of thermal transport in Li-ion cells, with particular emphasis on experimental measurements that advance the understanding of

fundamental processes. This review is organized into four major research directions: (a) temperature and thermal property measurements, (b) heat generation measurements, (b) thermal management, and (c) thermal measurements in runaway conditions. For each topic, key experimental measurement techniques are summarized and papers presenting pertinent data on materials and processes are discussed. Emphasis is given to more recent papers, within the last decade or so. A discussion on critical future research needs for thermal transport in electrochemical systems is also provided.

Thermal transport in Li-ion cells is still an evolving field, and it is expected that this critical summary will provide perspective of progress made so far, as well as pertinent future directions.

2 Temperature and Thermal Property Measurements

2.1 Temperature Measurement. Accurate measurement of temperature is key for all investigations of thermal transport in engineering systems. Traditionally, temperature of a body has been measured through linear transduction of temperature into another directly measurable physical quantity such as electrical resistance [29], thermal expansion [29], color [30], reflectance [31], circuit resonant frequency [5], etc. Key characteristics of any thermal measurement include measurement accuracy, measurement resolution, uncertainty, spatial resolution, and temporal resolution. These characteristics vary significantly from one measurement method to another, and also depend on the characteristics of the measurement instrumentation. For example, the electrical resistance-based thermometry has excellent measurement resolution when calibrated properly, but in general has poor spatial resolution unless microfabricated sensors are used. Calibration is critical in any temperature measurement approach.

Several specific challenges exist in temperature measurement for Li-ion cells and related systems. The need for in situ temperature measurements presents challenges due to the hermetically sealed nature of a Li-ion cell. Further, the electrochemically active environment makes it challenging to measure real-time temperature inside a Li-ion cell. It is not sufficient to merely measure the
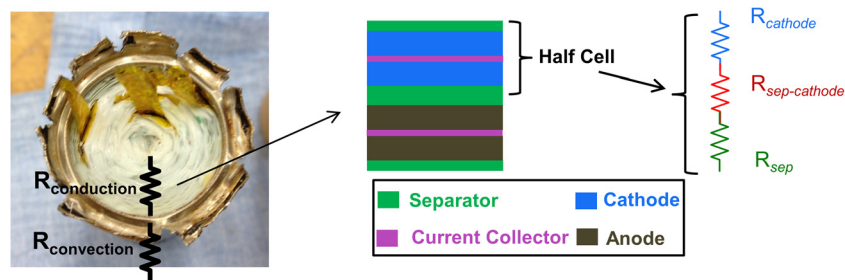
Fig. 3 Schematic of key thermal resistances in a Li-ion cell, and the breakdown of key material-level contributions. (Reproduced with permission from Vishwakarma et al. [55]. Copyright 2015 by Elsevier Publishing Company.)

outside temperature of a cell, since large temperature gradients are expected within the cell volume [24,25].

Several standard approaches for temperature measurement have been utilized for Li-ion cells and related systems. In addition, new, novel measurement techniques have also been used. Traditional thermometry techniques, such as thermocouples and infrared (IR) [32] imaging, have been used extensively to measure the surface temperature on a Li-ion cell. However, these approaches do not give any information on the temperature inside, which is expected to be significantly higher, hence more critical to measure [24,25]. It is important to note that due to low thermal conductivity of a Li-ion cell [33], the temperature inside a cell is unlikely to be single-valued, but rather a spatial field. Measurement of the internal temperature is also important to determine the temperature gradient within the cell, since a large gradient results in electrochemical imbalance. There are several difficulties in measuring internal temperature of a Li-ion cell. Accessing the core of a cell by drilling a hole to insert a thermocouple is in most cases not realistic, although it has been done for a limited number of test cells [34–40]. Thermocouple insertion has been carried out either during rolling/folding of the electrode stack [36,40], or by carefully drilling a hole in a commercial cell [34,35].
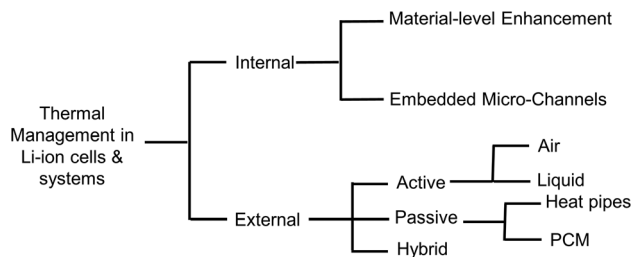
Thermocouple-based temperature and temperature distribution measurements inside a cell have been carried out at different discharge rates and at different convective cooling conditions [36]. In a similar work, the thermocouples have been inserted in a large-format laminated battery to examine temporal and spatial variation of the internal temperature [40].

Internal temperature of Li-ion cells has also been reported through several other mechanisms. These include measurement of temperature-dependent phase shift of voltage in response to a sinusoidal current [41–43], measurement of electrochemical impedance of the cell which is indicative of the internal temperature [39,44], and calculation of core temperature based on surface temperature using a lumped or reduced-order model [35,37,38].

It has been found that a sinusoidal current passing through a Li-ion cell results in a phase-shifted potential difference. In the 40 Hz–100 kHz range, this phase shift has been found to depend predominantly on the internal temperature of the cell [41–43]. This phase shift has been measured using a frequency response analyzer, which provides an indication of the internal temperature of the cell.

Some work has been reported on determining internal temperature of a cell by measuring the surface temperature and the electrochemical impedance of a cell [39,44]. This approach does not require knowledge of cell thermal properties, heat generation, or thermal boundary conditions but requires information on state-of-charge (SOC) of the cell. A calibration is performed in advance to relate temperature with the electrochemical impedance to be measured. This method has been shown to measure the temperature inside a cylindrical 26650 cell with a maximum error of 0.6 °C throughout the test [39]. Similar findings have also been reported for prismatic cells where a uniform temperature assumption is made [44].

Parameters required to calculate core temperature have been approximated using a lumped thermal model and reduced-order model approach. An online parameterization technique has been employed, which can determine these parameters as functions of state of charge, aging, and other degradations [35]. These parameters with [35] or without [37,38] online parameterization are then used to calculate the temperature of the core of the battery, which is compared against the measured value from a thermocouple inserted in the core of the battery [35,37,38]. A battery thermal model with constant internal resistance is explored first, which is later extended to address temperature-dependent internal resistance. This enables tracking of the long-term variation of the internal resistance. Note that this approach of using a lumped model ignores spatial temperature variation within the cell.

2.2 Thermal Property Measurements. The temperature field in any engineering system is governed by two key thermal transport properties—thermal conductivity, k, and heat capacity, C_p. While the thermal conductivity refers to the property of the material to conduct heat, the heat capacity refers to heat required to be added to a body for unit temperature rise. Thermal diffusivity α, defined as $\alpha = k/(\rho C_p)$, is also often measured for engineering systems. In addition to these material properties, the thermal transport is also often a strong function of thermal interface resistance between materials. While the heat capacity is a scalar quantity, in some systems, the thermal conductivity may be strongly direction-dependent. In Li-ion cells, the thermal conductivity anisotropy occurs due to the rolled/folded nature of the electrode stack. Both thermal conductivity and heat capacity are, in general, temperature-dependent, although in several cases, these properties may be nearly constants within the temperature range of interest. While the thermal conductivity is often measured through the temperature field resulting from an imposed heat flux or vice versa, the heat capacity is generally measured by determining the heat needed to be added for a specific temperature rise.

In the context of Li-ion cells, the thermal property measurements can be carried out at multiple spatial scales, including for individual materials of a Li-ion cell, such as separator, electrodes, etc., individual cells, as well as for larger systems. Thermal transport, particularly in larger systems, is also often characterized in terms of lumped thermal circuit parameters, including the thermal resistances and thermal capacitances of various components. Such an approach facilitates circuit representation and analysis of thermal behavior of systems.

Several experimental measurements, both of fundamental thermal conductivity and heat capacity, have been reported for Li-ion cell materials. Thermal property measurements are primarily done either at material level or at the cell level in Li-ion cells. At material level, the thermal property measurements of electrodes [45–49], electrolyte [50], separator [51,52], electrode stack [46,53], and contact thermal resistance [54,55] have been reported. Such material-level measurements are key in understanding the heat transfer inside a Li-ion cell and in determining the rate-limiting heat transfer processes.

Thermal property measurement of polymer electrolyte has been carried out using a guarded heat flowmeter [50]. Temperature difference across the sample is measured, which is used to calculate the total thermal resistance, from which the thermal conductivity of the polymer electrolyte has been extracted. Thin polymer electrolyte films are prepared by doctor blade technique and sandwiched between top and bottom plates, across which the temperature difference is measured. The thermal conductivity is reported to vary from 0.12 to 0.22 W/m K over a 25–150 °C temperature range [50].

Similarly, the thermal property of a composite cathode has been measured using a heat flowmeter [45]. The composite cathode is made of equal volume fractions of polymer electrolyte and a mixture of active material and acetylene black. The thermal conductivity of the composite is measured to vary in the 0.2–0.5 W/m K range between 25 °C and 150 °C [45].

Time-domain thermoreflectance (TDTR) has been used to measure the thermal conductivity of $LiCoO_2$ thin film. Effect of the

Fig. 4 Schematic of various thermal management strategies adopted for the cooling of Li-ion cells

degree of lithiation on thermal conductivity has been measured. In situ measurements of thermal conductivity of $LiCoO_2$ cathode during cycling show thermal conductivity to reversibly decrease from 5.4 to 3.7 W/m K when delithiated [47].

In-plane thermal conductivity of the separator material has been measured using a DC heating method [51]. Two thin metal lines, separated by a small distance, are microfabricated on the separator material. One of the lines is used as a heater, while both are used for temperature measurement. Ultrafast measurement of temperature of both lines as a function of time is used for determining the thermal properties of the separator. In-plane thermal conductivity and heat capacity of 0.5 W/m K and 2480 J/kg K, respectively, are reported at room temperature [51]. These values do not change significantly when measured at 50 °C.

Cross-plane thermal conductivity of electrodes and separators has been measured using a differential steady-state method [52]. The experimental setup is very similar to that of the 1D heat flow-meter previously used [45]. The cross-plane thermal conductivity of positive electrode (PE), negative electrode (NE), and separator is measured to be 2.0, 1.06, and 0.19 W/m K, respectively, in the presence of electrolyte [52].

Cross-plane thermal conductivity of several components and that of a stack of components have also been measured. The measurement is carried out using two different methods. In the first method, the thermal conductivity has been measured by ensuring 1D flow of the heat generated in the heater assembly passing through the NE–separator–PE stack. Values in the 0.33–0.66 W/m K range have been reported [46]. In the other method, the thermal diffusivity is measured using xenon flash technique from which the thermal conductivity is extracted using the heat capacity value measured separately. The out-of-plane thermal conductivity measurement of the stack is carried out at two different SOCs. The thermal conductivity measured for the stack is 1.90 W/m K and 2.36 W/m K, respectively, for the open circuit voltage (OCV) values of 2.45 V and 3.75 V. In the presence of electrolyte, these values change somewhat to 3.39 W/m K and 3.40 W/m K, respectively. The heat capacity was measured to be 1040 J/kg K and 960 J/kg K, respectively, for the OCV values 2.45 V and 3.75 V [46]. Similar work has been done to study the effect of cycling on thermal properties of lithium polymer cells [53]. Thermal conductivity and specific heat of the battery components taken out of from a fresh cell and a one cycled 500 times at 45 °C have been reported. The effect of cycling at high temperature on these parameters has been reported [53]. In-plane and cross-plane thermal conductivity of the anode material have also been measured using transient planar source and laser flash techniques [33,49].

In addition to these reports of thermal conductivity and heat capacity measurements, the thermal contact resistance between cell materials has been reported. In these experiments, the material stack is sandwiched between two copper blocks, and the total thermal resistance of the stack is measured. Key conclusions made here include lower contact thermal resistance of the wet stack compared to dry stack and weak temperature dependence of the stack resistance [54]. However, the thermal resistances measured here are the total thermal resistances which also include the material thermal resistance and not just the contact thermal resistances between the battery components. Contact thermal resistance between the electrodes and copper rods used in these experiments has been measured, which is not of particular relevance for in situ operation of the cell.

In another work, the interfacial thermal conduction between cathode and separator has been measured using a similar one-dimensional heat flow method. It has been shown that this interfacial resistance dominates over the material thermal resistances from the separator and cathode, offering around 88% of the total thermal resistance. This work concluded that the interfacial thermal resistance is the rate-limiting heat transfer process within a Li-ion cell and originates from the weak van der Waals adhesion between separator and cathode [55]. In addition to these material thermal characterizations, the cell-level thermal characterization

is needed to capture the nature of heat transfer phenomena at the spatial scale of a cell. There have been a few experimental measurements reported in literature for the cell-level thermal property measurements. Some of these are based on primarily thermal methods [56–59], whereas others are based on the coupling between thermal transport and electrochemical properties [60,61]. It is important for such measurements to account for anisotropy due to the rolled/folded nature of the electrode roll. Lumped and reduced-order model-based thermal parameter characterizations have also been done [35,37,38].

An analytical solution-based approach has been used where a Li-ion cell is externally heated and the measured transient temperature rise is fitted with an analytical solution to determine the thermal conductivity and specific heat. The radial thermal conductivity is measured to be 0.15–0.2 W/m K for 26650 and 18650 cells. Axial thermal conductivity measurements show the axial thermal conductivity to be 30.4–32.0 W/m K, which represents nearly 150-fold anisotropy [57]. This work also allows simultaneous heat capacity measurement which is determined to be 1605–1720 J/kg K for 26650 and 18650 cells [57]. Another paper with a similar approach reports similar values for thermal conductivities, but a much lower heat capacity, in the range of 814–972 J/kg K [58].

The axial thermal conductivity of a Li-ion cell has also been measured using a comparative method to obtain the heat flow through a battery indirectly, while preventing heat loss via thermal compensation [56]. The thermal compensation system consists of a heater which reduces the radial temperature gradient to minimize the radial heat losses. This method is difficult to adapt for radial thermal conductivity measurement. In this work, the radial thermal conductivity was estimated to be around 1.0 W/m K from the known thermal conductivities of the electrode stack components, ignoring the thermal contact resistances. Axial thermal conductivity was reported to range from 6.83 to 4.25 W/m K over an entire discharge process [56].

The specific heat capacity and cross-plane thermal conductivity for a 75 Ah lithium iron phosphate (LFP) pouch cell have been measured using an isothermal calorimeter. The influence of SOC and temperature on the specific heat capacity of the LFP cell is considered in modeling and calculations. Over the full temperature range from −5 °C to 55 °C, this property is found to vary by approximately 38%. The cross-plane thermal conductivity is reported to be around 0.42 W/m K and nearly independent of temperature across the full SOC range [59].

The thermal impedance spectrum of a system—analogous to electrochemical impedance spectrum (EIS)—has been used to provide information about the thermal properties of the system [60,61]. The thermal impedance is measured through Laplace transform of the transient temperature rise in response to an external or internal heat pulse. The thermal impedance spectra have been obtained for batteries from different manufacturers and used as validation of this method. The heat capacity and thermal conductivity are obtained from a nonlinear fit of the experimental data with a theoretical impedance function developed for a cylindrical rod with external heat generation. Heat capacity and thermal conductivity of the electrode roll of an 18650 Li-ion cell are measured to be 1900 J/kg K and 1.4 W/m K, respectively [60]. However, anisotropy in thermal conductivity is not accounted for here. The effect of SOC has also been studied for one of the cells, which indicated slight increase in the thermal conductivity with state of charge [60]. Using a similar technique, the thermal conductivity and heat capacity of a 4.4 Ah $LiFePO_4$ cell have been reported to be 0.35 W/m K and 958 J/kg K, respectively [61].

3 Heat Generation Rate Measurements

Temperature distribution inside a Li-ion cell plays a crucial role in determining the performance, safety, and life of the battery. The temperature distribution in a Li-ion cell is determined by heat generation and heat dissipation processes. While heat

dissipation can be understood by measuring the thermal properties discussed in Sec. 2.2, it is also important to understand and quantify the source of heat generation in the cell, and relate it to electrochemical parameters such as C-rate and cell electrochemical impedance. Heat generation in a Li-ion cell comprises reversible and irreversible components [10,17,62–67]. Reversible heat generation occurs due to entropic changes in the battery, whereas irreversible heat generation is caused by numerous events such as Ohmic losses, mass transport, charge transport, and interfacial kinetics [17]. A large body of research exists on coupled electrochemical–thermal modeling of heat generation through theoretical and numerical methods. [62–64,68,69]. On the experimental side, two common tools—accelerated-rate calorimetry (ARC) and isothermal heat conduction calorimetry (IHC)—have been used for heat generation measurement [17,70]. In ARC, heat generation is measured by measuring the amount of heat dissipated by the battery to the surroundings and the temperature rise of the battery. On the other hand, in IHC, the measurements are carried out in isothermal conditions, maintained using heat sinks in contact with the battery surface. In IHC, heat generation within the battery is measured by means of a heat flux sensor located between the battery surface and the heat sink. In the past two decades, ARC and IHC have been used extensively for heat generation measurement in Li-ion battery [65,67,71–81].

One of the earliest reports of ARC-based electrochemical–calorimetric measurements for Li-ion cells was in 1998 [65]. In this work, the voltage, current, and temperature were measured at different charge/discharge rates while an 18650 cell was inside a calorimeter [65]. This methodology has been extended to a number of other commercial Li-ion cells [67]. In a related study, a similar experimental setup has been used for measuring change in heat generation rate due to structural transformation in the graphite anode and phase change of the $LiCoO_2$ cathode [74].

Many papers have also reported heat generation measurement based on IHC [71–73,75–81]. An experimental investigation on using IHC for heat generation measurement of $LiMn_2O_4$ cathode-based prismatic cells has been reported [81]. An aluminum vessel has been attached on the cell surface to maintain the isothermal conditions. The vessel also acts as a current collector for anode. Calvet-type conduction microcalorimeter has been used to measure the heat flow during charge/discharge [81]. Heat generation measurement on coin cells during charge and discharge has been reported using an isothermal calorimeter. Data on three different coin cells with different cathode and anode composition have been reported [72]. Later, the heat generation measurement of mesocarbon microbeads (MCMB) in an MCMB/Li cell using isothermal microcalorimeter has also been reported [77].

ARC and IHC are both inherently ex situ in nature, since the cells need to be isolated inside a calorimeter. Most ARC and IHC measurements are also limited to low and moderate C-rates on small-sized cells. There is relatively less literature on in situ measurements at high C-rates. ARC and IHC have been reported to be more accurate in maintaining temperature uniformity for smaller geometries compared to bigger ones [66]. This might be a possible reason behind lack of research on heat generation measurement at pack level. Recently, a thermal technique based on measurement of heat stored through internal temperature measurement and measurement of heat lost through a heat flux sensor has been used for in situ heat generation measurement in Li-ion cells at higher C-rates up to 9.6C [34]. In this method, the measurements are carried out during the normal operation of the cell, without the need of a calorimeter. These measurements are in good agreement with a separate, IHC-based heat generation rate measurement at high C-rates on a similar cell [66].

4 Thermal Management Approaches

Thermal management has been an active area of research for a wide variety of heat-generating engineering systems such as nuclear fuel rods, microelectronics, etc., where heat generated

during operation must be effectively rejected to the ambient in order to limit the temperature rise of the system. Excessive temperature rise presents safety and reliability concerns, and in most cases, performance reduction as well. For systems with low heat generation, passive cooling by heat loss to the ambient may be sufficient. As the heat generation rate increases, the thermal management system becomes more and more sophisticated. Options for advanced thermal management include two-phase liquid cooling, nanomaterials-based cooling, etc. Thermal storage is also a promising opportunity, for example, for addressing transient peaks in heat generation, which is particularly relevant for high-rate discharge automotive applications of Li-ion cells where a large amount of heat may be generated in a short pulse. In addition to system design, run-time thermal control is also critical for implementing measures to modulate active thermal management algorithms such as load balancing and throttling to manage cell temperature as a function of time. The thermal management strategies vary in terms of complexity, cost, and performance. The thermal management for Li-ion cells must be recognized at multiple length scales—materials, cells, and systems. A key metric of performance is the total temperature difference between the point of heat generation to the ambient, expressed per unit heat transferred, often referred to as the total thermal resistance. However, for spatially distributed heat generation, as is the case for a Li-ion cell, it is not sufficient to define a total thermal resistance. Instead, fundamental thermal properties such as thermal conductivity of the Li-ion cell need to be known, based on which the temperature field inside the cell can be determined. Further, the thermal resistance concept is inherently steady-state only, and to capture transient effects, the heat capacity of the cell must also be known.

Figure 4 schematically shows a classification of various thermal management strategies that have been adopted for Li-ion cells.

4.1 Material Thermal Management. While materials of Li-ion batteries are well optimized for electrochemical performance, relatively less work has been reported to measure and optimize material-level thermal transport. Figure 3 shows that the thermal unit cell is a Li-ion cell electrode–separator roll and key thermal resistances therein. A limited amount of work has been reported on enhancing these thermal resistances. Among materials, the separator has the least thermal conductivity, around 0.5 W/m K [51], and attempts have been made to improve its thermal conductivity. A hierarchical nano/micro-Al_2O_3/polymer separator with improved thermal conductivity of 1.0 W/m K has been developed, without ionic conductivity [52]. Material-level enhancement of $LiFePO_4$ cathode has been carried out to improve the thermal diffusivity by using carbon-coated cathode and organic binders [82]. In a related work, the thermal conductivity of $Li[Ni_{1/3}Co_{1/3}Mn_{1/3}]O_2$-based cathode has been enhanced by two orders of magnitude by capturing the cathode materials inside the multiwall-carbon nanotubes matrix [33]. Similarly, work has been done to improve the thermal conductivity of the anode material [48].

Recent work has shown that the thermal contact resistance between separator and cathode may contribute up to 90% of the total thermal resistance of the thermal unit cell. This dominant, rate-limiting thermal conduction process has been improved by chemical bridging protocol of the interface, resulting in improved surface adhesion and a measured 4× reduction in thermal contact resistance [55].

In addition to enhancement of material and interfacial thermal conduction, internal cooling by flow of R134a through microchannels integrated inside current collector has also been proposed as a thermal management approach. To demonstrate this, a surrogate heat source is used to simulate battery heat generation, and an aluminum plate is used with embedded microchannels to represent the internal cooling in current collectors [83]. Similar concept has been investigated by carrying out 2D and 3D transient thermal analyses for cooling the prismatic cells by making the liquid

electrolyte flow through the internally embedded microchannel [84].

4.2 External Thermal Management

4.2.1 Air Cooling. Air cooling of Li-ion cells is relatively easy to implement, but has limited thermal effectiveness. Air cooling can be carried out passively through natural convection, or actively through forced convection. Much research has been carried out in developing mathematical thermal models and validation through numerical simulation [85–90]. The concept of reciprocating air flow model in a lithium-ion battery pack for better temperature uniformity by varying the air flow direction has been proposed. Later, a numerical analysis for various air cooling configurations for a hybrid electrical vehicle (HEV) battery pack has been carried out [85–87]. In a related work, thin duct design for cooling based on distributed natural convection has been investigated [86]. Thermal analysis of the proposed battery pack is done by solving the governing energy equations and boundary conditions that describe the temperature distribution in the battery pack [86,87]. However, these papers lack experimental implementation.

Experiments for air cooling a high-capacity lithium–titanate battery pack of 50 Ah cells have been performed. Blowing ambient air between the cells results in low heat transfer coefficient; therefore, the metal-foam based heat exchanger has been proposed. Al-based metal foams are placed between five cells and compressed with metal plates from the sides. Air inlet and outlet are provided at the top and bottom, respectively. With this arrangement, the temperature rise of the battery has been limited to 10 °C even when discharged at 200 A [91]. The thermal and fluid flow field characteristics of 55 Ah lithium-ion battery system for different air duct modes have been also investigated. It has been shown that U-shaped ducts are more effective in heat dissipation for different SOC state, ambient temperature, charge, and discharge rates [92]. Effectiveness of the cooling strategies is found to be dependent on cell arrangements and orientation [93,94]. Two-dimensional air flow in 12 CA180 cells arranged in two rows with cooling ducts has been studied. Cooling plates are attached on the sides in this closed module and two fans are provided for air flow. Cooling ducts allow air flow between cells. Two-dimensional air flow configuration at 1C discharge rate resulted in 9 °C reduction in maximum temperature of the pack compared to the baseline case with no cooling strategy [93]. The thermal performance of a lithium ion battery pack with five different arrangements of 25 cells has been also reported. All cells were enclosed in a module with fan on one side and vent on the other. A 5 × 5 cubic structure is found to be best in terms of cooling capacity, and a 19-cell hexagonal arrangement is found to be best for space utilization along with cooling effectiveness [94].

4.2.2 Liquid Cooling. Liquid cooling can be an effective mechanism for active thermal management of lithium ion battery systems. Water is often chosen as the working fluid due to excellent thermal properties and low cost. However, it is critical to minimize risk of leakage and electrical damage. For this reason, dielectric fluids may also be a good choice. Many theoretical and numerical models on liquid cooling plate design, optimization, and cooling strategies for battery packs have been developed [83,95–102]. The serpentine cooling plate design for electric vehicle battery pack has been modeled and optimized [100,101]. A numerical model has also been developed to understand the effect of cooling plate thickness and coolant velocity under forced liquid cooling [97].

Liquid cooling plates are the most common form of active mode cooling strategies being investigated for battery systems. Cooling plates can be inserted between the battery/battery packs and the coolant can be cooled externally [98]. Cold plates often have fabricated microchannels with internal coolant flow [95,99]. Oblique fin microchannel cold plates placed between two batteries have been investigated. The effect of one inlet/outlet and two inlet/outlet configuration on maximum temperature of the system is presented for different flow rates. Improved temperature uniformity has been reported for oblique fin cold plate compared to the straight cold plate arrangement [95]. Straight microchannel cold plate design has been investigated, where the cold plates are sandwiched between batteries with inlet and outlet at opposite ends. The number of microchannels is varied, and the extent of cooling is found to increase with the number of microchannels. At 5C discharge rate, this work also reports that there exists an optimal flow rate beyond which the system efficiency decreases. Liquid cooling has been also investigated for external passive cooling by using ethylene glycol–water as coolant. A single pack of battery module with cold plates on the sides is considered in this work. The maximum temperature has been limited to 35 °C at 2.375 l/min flow rate. The experimental data show good agreement with the numerical model with <2 °C deviation in maximum temperature [98].

Several other cooling strategies utilizing a low boiling point liquid have also been demonstrated [103,104]. The cooling of a module of ten batteries with spacers made of porous material has been experimentally investigated. The entire module is submerged into a low boiling point dielectric liquid. Evaporated liquid is condensed in a heat exchanger and is pumped back to the module [103]. In a separate study, a piston-based mechanism has been investigated for improved control over the boiling process and better temperature uniformity [104]. It has been shown that the 0.7 °C temperature difference between the positive and negative terminal in the nonboiling regime can be completely eliminated, once the battery is under the liquid boiling process [104].

4.2.3 Heat Pipes. Heat pipes have been widely used in industrial applications and academic research for improved thermal management and other advantages such as space efficiency [105,106]. While the physics of heat pipe operation is remarkably complicated, involving multiple coupled phenomena such as phase change, fluid flow, etc., the implementation is relatively straightforward. A 2D transient thermal model for heat pipe cooling of a 12 Ah cylindrical battery has been proposed [90]. In this work, heat pipes are placed on two annular aluminum fins, and the condenser part of the heat pipe is cooled by natural convection and forced convection. Significant reduction in the temperature rise is reported for high discharge currents [90]. An experimental investigation of prismatic cells with heat pipes has been also presented [107]. Copper heat pipes are sandwiched between the two cells and the condenser part is cooled by a constant temperature water module. For different heat generation rate (<50 W), maximum temperature rise on the battery has been limited to within 50 °C [107]. Similar work with oscillating heat pipes instead of copper heat pipes has been discussed in this review article later [108]. Experiments with L-shaped heat pipe inserted between the battery cell cavity between four Li-ion cells have been carried out. Glycol–water mixture has been used for removing heat from the condenser part of the heat pipe. It has been shown that for 10 W/cell heat generation, the surface temperature can be maintained at 40 °C. The surface temperature at 4C discharge is reported to be 10 °C less compared to the case when no cooling strategy is implemented [109].

Shape and orientation of heat pipes play a key role in heat removal and have been studied experimentally for different Li-ion battery systems of electric vehicle (EV) applications [110–112]. The heat pipe design and prototype for a specific EV lithium-ion battery module have been proposed. Heat pipes are attached to the condenser section with a bend of 121 deg. The condenser is provided with aluminum fins which are cooled by forced convection [110]. In another work, a surrogate heat source is used to represent the HEV battery module, and flat heat pipes are attached to the sides. The condenser part of the heat pipe is then attached to an aluminum heat sink which has been cooled by blowing air [111]. Flat heat pipes have also been used for cooling of 3 Ah and 8 Ah pouch Li-ion battery packs. A flat heat pipe is sandwiched

between batteries, and condenser end is cooled by natural convection, forced convection, thermostat bath, and wet cooling. Temperature rise has been limited to less than 4 °C for a 3 Ah pack discharging at up to 4C. Wet cooling has been reported to be more effective in heat removal for the heat pipe arrangement considered in this work [112].

Pulsating heat pipes (PHPs) and oscillating heat pipes (OHPs) are relatively recent modifications of the conventional heat pipe [108,113]. The PHP/OHP consists of a plain serpentine tube of capillary dimensions with many U-turns. In contrast to a conventional heat pipe, there is no additional capillary structure inside the tube. PHPs and OHPs have been investigated for the cooling of Li-ion battery packs. Heat dissipation has been studied for four different working fluids and at different heat generation ranges (25–550 W) [113]. Cooling of prismatic cells has also been investigated. The experimental setup uses four-turn loop OHP with condenser at top and evaporator at bottom. The evaporator part is sandwiched between the two batteries. The condenser is being cooled by a constant temperature water bath. Vertical arrangement of the battery along the OHP has been reported to be more efficient in reducing the overall maximum temperature compared to the horizontal arrangement [108].

4.2.4 Phase-Change Material (PCM) Thermal Management. Phase-change materials (PCMs) have been widely used for heat and cold storage in various fields [114–118]. In the past two decades, PCMs have been investigated for thermal management of Li-ion battery systems. PCMs are excellent in cooling the Li-ion cell/pack by absorbing transient spikes in heat generation. The stored heat can either be dissipated to ambient efficiently, or can be used to maintain the optimal temperature of Li-ion battery system in cold climates. Salt hydrates and paraffin-based PCMs are the most commonly used phase-change materials used in Li-ion cell cooling [118]. In an early work, the paraffin-based PCM has been filled between eight 10 Ah batteries of an EV battery pack, which acted as a thermal sink for generated heat. Further, the stored heat has been utilized to keep the battery above room temperature, thereby increasing the overall energy efficiency of the battery system [119]. Later, the numerical simulation of PCM-based cooling of a Li-ion battery system for electric scooter has been developed [120]. This design has been experimentally tested for a pack of 18650 2.2 Ah Li-ion cells [121]. This work includes cooling of the battery pack by natural convection, Al foam between the cells, PCM between the cells, and a combination of PCM and Al matrix. Results show that PCM-based cooling significantly reduced the temperature rise compared to the case of natural convection alone [121].

PCMs offer several advantages such as high latent heat, compactness, and good cycling stability. However, a key drawback is the poor thermal conductivity. Several studies have been reported where the thermal conductivity of PCM has been enhanced by impregnating with particles/fillers of high thermal conductivity [122]. The numerical simulation on Li-ion laptop battery pack with PCM for thermal management has been carried out. In this work, the paraffin wax-based PCM has been modeled, and the concept of a composite of PCM and expanded graphite (EG) has also been introduced. Simulation results have shown that operating temperature can be kept <50 °C for high discharge rate by doubling the amount of PCM [123]. In order to implement this idea in Li-ion battery system, a composite of EG and paraffin-based PCM has been prepared, and a very high thermal conductivity (16.6 W/m K) compared to pure paraffin-based PCM (0.2 W/m K) has been reported [122]. In a similar study, PCM/EG composite blocks for Li-ion battery have been prepared and their thermomechanical properties have been studied [124].

Graphene-enhanced hybrid PCMs for thermal management of Li-ion batteries have been proposed. The thermal conductivity is reported to be 60 times higher than paraffin. In this work, a pack of six 3 Ah Li-ion cells surrounded with hybrid graphene–PCM is investigated. Graphene-enhanced PCM resulted in 10–16 °C less

temperature rise compared to the conventional PCM [49]. In a related work, the graphite sheets in external contact with PCM/EG composite have been used. A graphite sheet is sandwiched between the two batteries, and the two ends are attached to the PCM/EG blocks. Maximum temperature rise for the pack at 1C and 2C discharge is reported to be less than 5 °C compared to the case where the PCM-based thermal management strategy is not used [125]. Use of carbon fibers in PCM to enhance thermal conductivity without sacrificing the latent heat capacity has been also reported. This work reports 45% reduction in the maximum temperature in 4C rate discharge condition [126].

4.2.5 Hybrid Thermal Management. Coupling passive thermal management strategies with active cooling systems has been of much recent interest [127,128]. Experimental investigation with PCM-based thermal management system in conjunction with active water cooling has been carried out. In this study, a 27-cell module of 26650 cells has been inserted in an aluminum can filled with liquid PCM and covered with water-cooled copper plates at top and bottom. PCM solidification at 2C charge rate after the discharge driving cycle has been successfully demonstrated in this work [127]. In a related work, PCMs have been integrated with forced air cooling. Forced convection is used to remove the accumulated heat of PCMs in a pack of 20 18650 cells [128].

5 Thermal Runaway Characterization and Measurements

Li-ion cells are remarkably temperature-sensitive, and the behavior at elevated temperature presents serious safety concerns. At temperature greater than a threshold value, a series of exothermic processes are known to occur, with heat generated from one activating the next set of processes, effectively generating a thermal runaway situation. Pertinent processes here include decomposition of solid electrolyte interface (SEI) layer, reaction of negative electrode with electrolyte, unstable PE material, electrolyte combustion, dendrites formation, melting of separator, electrolyte decomposition, oxidation of organic solvents, etc., which result in pressure buildup inside the cell, fire, and ultimately explosion [18,19,129–131]. These processes typically follow Arrhenius reaction dynamics, causing exponential increase in heat generation rate with increasing temperature. This potentially leads to a thermal runaway situation when the heat generated by the cell cannot be effectively removed, and thus results in ever-increasing cell temperature [19,132].

Several factors leading to initiation and progression of thermal runaway have been investigated by understanding the thermal stability of different components in a Li-ion cell [133]. Individual materials such as cathode active material, anode, and electrolyte also been studied to understand their contribution toward over thermal instabilities of batteries [133–139]. Some alternative materials and modification to the existing materials for the cathode active material, anode material, salt in the electrolyte, and modifications to the separator have also been proposed due to their higher thermal stability under abuse conditions which would lead to safer Li-ion cells [134,140–145]. Thermal runaway inhibitors and flame retardants have also been used as additive to electrolyte to improve the thermal stability and reduce the possibility of fire and explosion in Li-ion cells [146,147]. Different abuse conditions and their effect on overall stability of the Li-ion cell have been studied by simulating various possible abuse conditions such as internal short circuit, overcharge, high temperature, and physical abuse [148–152].

5.1 Cell-Level Thermal Abuse Measurements. Thermal abuse performance of a variety of Li-ion cells has been investigated by inducing thermal runaway through a variety of mechanisms such as overcharging, nail impact, etc. The short circuit and overcharge behavior of prismatic lithium-ion batteries containing $LiCoO_2$ cathodes and graphite anodes have been reported [148].

Internal thermocouples have been used to characterize the thermal profiles of the cells under abusive conditions. During short-circuit test, the cell remained sealed and reached an internal temperature of 132 °C, but did not enter thermal runaway. On the other hand, an extreme overcharge testing was found to lead to different outcomes depending on the current used to charge the battery. The cells get ruptured at higher currents during overcharge test. Melting of lithium has been found to be the underlying factor leading to the rupture of the cells [148].

Similarly, an internal short circuit has been simulated in prismatic Li-ion and Li-ion polymer (LIP) cells [149]. In cells with higher capacity, the risk of thermal runaway has been found to be higher from internal short circuits due to higher temperature at the short-circuit site and the surrounding region, which could approach the separator melting point and the decomposition reaction temperature of cathode material [149].

Work has been reported on systematic internal short-circuit tests on cells using a well-controlled pinch test [150]. With this pinch test, reproducibility in creating 1–2 mm size internal short circuit in one or two inner layers of a cell anode and cathode has been demonstrated. This possibly mimics the type of internal short circuit which may occur in real conditions. These tests also show that the risk of thermal runaway during internal short circuit increases with increase in the cell's state of charge and capacity, which is consistent with the previous findings [150].

Some more work has been done in improving the methodology for an internal short-circuit test to make it more representative of realistic short circuit [151]. This includes the use of an embedded metal or metal alloy trigger inside the cell, which has been electrically isolated when solid but melts when externally triggered and shorts the electrodes [151]. Heat required to trigger this short circuit is moderate and does not by itself cause significant temperature rise of the cell.

One more standard test in battery testing is the nail test in which a metal nail is pierced at center of a battery with certain nail speed. This causes internal electrical short circuit in the battery [153]. Nail test has been performed on a fully charged 100 Wh battery. A motor mechanism has been used to penetrate a sharp stainless steel nail into the center of the cylindrical battery body with a speed of 1 mm/s. Slight insertion of nail immediately results in opening of two safety vents, which is then followed by large volume of electrolyte vapor jet coming out from the vents. The surface temperature of the battery reaches a maximum temperature of 380 °C in very little time [153]. This rapid temperature rise occurs due to the abrupt conversion of the stored energy in the cell into heat due to internal short circuit caused by the nail.

A thermal abuse model that predicts single-cell behavior at elevated temperature has been utilized to characterize the effect of temperature-dependent exothermic reactions [154]. Thermal runaway has been triggered using a constant-power heating element. Reasonable agreement has been shown between the experimental data and the model predictions. Effect of convection, cell physical configuration, and electrolyte combustion on the cell thermal behavior has been analyzed using the model [154].

More sophisticated theoretical modeling tools have also been developed and validated with the experimental simulation of thermal runaway [155,156]. A three-dimensional thermal abuse model for high-capacity Li-ion batteries has been developed based on finite element method [155]. During oven test simulation, nonuniform temperature distribution in the cell has been observed. The model has been shown to predict the qualitative and quantitative behavior of a cell in an oven test with reasonable success. Similarly, an experimentally validated numerical model has been developed to predict the temperature response of a cell during oven test [156]. This model uses already developed reaction kinetics and thermal properties from the literature to predict the temperature response of cells of various designs and anode materials. The model also predicts the onset of thermal runaway by simulating oven test at elevated temperature.

The role of radiation in enhancing the effective heat dissipation to the surrounding during thermal abuse condition is also studied [157]. In this work, it has been reported that as much as 50% of the total heat dissipation can happen by radiation at elevated temperatures. The label, wrapped around a Li-ion cell, is shown to be critical for effective heat dissipation by radiation.

Finally, some work has been done in understanding the thermal runaway and its propagation in a battery module. Experimental measurements and theoretical analysis have been done on different battery module configurations to characterize the thermal behavior and determine the safe practices [158]. A single cell in a module is triggered into thermal runaway by heating it up, and the cell-to-cell thermal runaway propagation behavior has been characterized. Based on the experimental results and theoretical analysis, it has been shown that increasing the intercell spacing in a module containing cylindrical cells significantly decreases the probability of thermal runaway propagation. Role of tab configuration and cell form factor has been also shown to have a major influence on the thermal runaway propagation. Effect of different thermal insulation materials to contain the propagation of thermal runaway has been analyzed using the theoretical analysis. In another work, the cell-to-cell failure events and propagation in lithium-ion batteries have been studied using 18650-type $LiCoO_2$ lithium-ion batteries and several inactive surrogate cells fitted with thermocouples and/or cartridge heaters. Both single cell and multicell packages have been tested to study the response during a typical failure event, and the analysis of these studies has been used to understand the heat propagation to neighboring cells before, during, and after the event [32].

5.2 Material-Level Thermal Runaway Measurements. A number of experiments have been carried out to understand the material-level processes that contribute to thermal runaway. Thermal stability of fully charged 550 mAh prismatic Li-ion cells (Sn-doped $LiCoO_2$/graphitic carbon) and their components has been investigated [133]. Using the accelerating rate calorimetry (ARC), the onset temperature of exothermic chemical reactions has been determined, which could force the cell into thermal runaway. Based on the differential scanning calorimetry (DSC) and thermogravimetry, the thermal stability of the cell's positive electrode (PE) and negative electrode (NE) materials from 35 to 400 °C has been analyzed. The cell's self-heating exothermic reactions have been found to start at 123 °C, which eventually leads to thermal runaway near 167 °C. The total exothermic heat generation of the NE and PE materials is 697 and 407 J/g, respectively. These heat generation rates show significant reduction when the materials are washed in diethyl carbonate (DEC) and dried below 65 °C under vacuum [133].

Li_xCoO_2, Li_xNiO_2 and $Li_xMn_2O_4$ (x < 1) are considered metastable and known to liberate oxygen when heated in air or in inert gas. The temperature at which oxygen evolution occurs depends on the value of x and on the compound. Thermal decomposition of these compounds has been studied in inert gas using the thermal gravimetric analysis and mass spectrometry. Among the three, nickel compounds are found least stable whereas the manganese compounds are most stable. The cobalt compounds exhibits intermediate stability. These results have important implications for the safety of Li-ion cells as the commonly used cathode active material $LiCoO_2$ has been shown to be not as thermally stable as $LiMn_2O_4$ [135]. Similar conclusions have been also made based on safety tests, such as heating, overcharge, nail penetration, and forced discharge test performed on 600 mAh class commercially available prismatic where $LiMn_2O_4$ has been found safer to be used in Li-ion cells than $LiCoO_2$ [134].

Thermal runaway features of a 25 Ah large-format prismatic lithium ion battery with Li ($Ni_xCo_yMn_z$) O_2 cathode are evaluated using the extended volume-accelerating rate calorimetry [137]. Thermocouples are inserted into the battery at different locations. The temperature inside the battery has been measured to be

870 °C, which is much higher than the temperature measured at the outer surface of the battery. Temperature has been observed to rise to approximately 520 °C when the thermal runaway happens. The temperature rise reported in this paper appears to be somewhat high. The temperature rise follows sharp drop in the measured voltage of the battery which happens 15–40 s prior to the instantaneous rise of temperature. This time interval can serve as an early warning of the thermal runaway.

A 720 mAh Li-ion cell has been tested for overcharge using soft overcharge technique [136]. This technique has been used to follow the overcharge process gradually and thoroughly to investigate the stage which can be considered most critical and irreversible. The characteristics of the battery material at different overcharge stages have been evaluated by performing DSC and scanning electron microscope tests.

Growth of cathode microparticles has been reported on anode side of the surface of a separator recovered from an overcharge test. This indicates that growth of microcathode particles penetrating through separator might play a key role in producing a microshort that ultimately leads to thermal runaway. However, SEI layer breakdown, which happens in temperature range of 120–130 °C, could also be considered as a trigger for full cell thermal runaway followed by the microshorting phenomena described earlier [136].

The thermal behavior of the natural graphite anode at different states of charge has been studied using DSC [138]. Anode samples with more intercalated lithium produce broad DSC peaks following SEI film decomposition, which is also attributed to the formation of a secondary SEI film. Decomposition of SEI films gives out an exothermic peak. Another sharp exothermic peak has been observed, attributed to the structural collapse of graphite at high temperatures for sample with more than 0.71 lithium per graphite. Due to the collapse of graphite, Li releases from graphite particle which reacts with the polyvinylidene difluoride to produce more heat. The thermal stability of the graphite anode improves when it is made up of carbon-coated spherical graphite particles [138].

The thermal stability of lithium hexafluorophosphate ($LiPF_6$) in Li-ion battery solvents has been studied using the thermogravimetric analysis and online Fourier transform infrared (FTIR) [139]. There has been no evidence found of thermally induced reaction between $LiPF_6$ and typical Li-ion battery solvents. However, this is in the absence of any impurity such as alcohol or the cathode material, which is expected to act as a catalyst and cause some undesirable reactions [139].

Thermal stabilities of different lithium salts and the roles of the salts on the thermal behaviors of their based electrolytes have been studied. For the salts: lithium hexafluorophosphate ($LiPF_6$), lithium tetrafluoroborate ($LiBF_4$), lithium bis(trifluoromethylsulfonyl)imide (LiTFSI), and lithium bis(oxalato)borate (LiBOB), there has been no exothermic behavior noticed. The mixture systems are relatively thermally stable in the absence of lithium salts. The thermal stability of solvents reduces significantly in the presence of lithium salt, especially in the case of $LiPF_6$ salt. However, LiBOB-based electrolyte has been reported to show excellent thermal stability [159].

5.3 Material-Level Enhancement for Improved Thermal Runaway Performance. Advances have been made in improving thermal stability of the anode and cathode materials [140–142]. Two advanced cell chemistries called Gen1 and Gen2 have been developed [140]. Gen1 cells consist of an mesocarbon microbeads (MCMB) graphite-based anode and a $LiNi_{0.85}Co_{0.15}O_2$ cathode material, while the Gen2 cells consisted of a MAG10, a type of graphite, anode, and a $LiNi_{0.80}Co_{0.15}Al_{0.05}O_2$ cathode. The thermal response and properties of the cells and cell materials are measured using ARC and DSC for temperatures up to 400 °C. Gen1 cell chemistry has been found to be thermally stable, which is credited to the MCMB graphite as it enables more effective solid electrolyte interface (SEI) formation. On the other hand, Gen2 cell chemistry with Al stabilized cathodes is observed to have higher peak reaction temperatures, which also results in improved cell thermal stability. The thermal stability of these cells seems to increase with aging due significant reduction in exothermic heat generation at the anode.

A new cathode material with concentration-gradient structure within each particle's outer layer has been developed [141]. This material shows a very high reversible capacity of 209 mAh/g based on the particle bulk composition of $LiNi_{0.8}Co_{0.1}Mn_{0.1}O_2$ and also improved cycling and safety characteristics. These enhanced characteristics are attributed to the stability of the concentration-gradient outer layer and the surface composition of $Li[Ni_{0.46}Co_{0.23}Mn_{0.31}]O_2$.

Thermal stability of Li-ion cells that use Sb and intermetallic Cu_2Sb as anode has been investigated and compared to conventional graphite electrode cells [142]. X-ray diffraction (XRD) and X-ray photoelectron spectroscopy (XPS) have been used for ex situ characterization of bulk and surface layer products of the thermal reactions. Using the differential scanning calorimetry (DSC), the relative heat generation with these electrodes has been measured. Reduction in the low-temperature exothermic is observed, which turns out to be the driving force for thermal runaway. The heat generation per unit capacity for both Sb and Cu_2Sb is reported to be approximately 37% lower than graphite [142].

Some work has been done to improve the thermal stability of the separator [143,144]. The micropore surfaces in the polyolefin-based separator have been fully covered by a thin layer of SiO_2 deposited by chemical vapor deposition [143]. This results in significantly enhanced thermal stability of the microporous separators. No adverse effect on ionic conductivity has been reported. The thickness of the SiO_2 layer is found to be a crucial parameter which could result into separator with high stability at high temperature and uncompromised cell performance.

Similarly, microporous polyacrylonitrile (PAN) nonwoven separators have been developed by using electrospun nanofibers with homogeneous diameter of 380 and 250 nm [144]. Cells with these separators have been reported to exhibit better cycle lives and higher rate capabilities than that of a cell with conventional one. These separators are shown to be thermally stable at 120 °C.

The volatile nature of traditional organic electrolytes has been considered to be a key reason in fire caused under abuse conditions. An improved salt lithium oxalyldifluoroborate (LiODFB) with combined advantages of LiBOB (lithium bis(oxalato)borate) and $LiBF_4$ has been made [145]. Its chemical structure comprises the half molecular moieties of LiBOB and $LiBF_4$. The salt is also noted to be highly capable of stabilizing solid electrolyte interface (SEI) on the surface of graphite anode. This enables Li-ion cell to be operated at high temperature without the risks posed by the convectional electrolyte. The electrolyte made with this salt undergoes thermal decomposition at approximately 240C which is 40C higher than the $LiPF_6$ [145].

To improve the thermal stability of electrolyte, and hence the overall thermal stability of a Li-ion cell, the thermal runaway inhibitors (TRIs) have been identified, prepared, and used as an additive (2–5%) to the standard battery electrolyte system; these materials improve the safety by preventing potential fire and explosion [146].

Some others additives such as trimethyl phosphite and trimethyl phosphate have also been added to the electrolyte additives to improve the safety and electrochemical performance of lithium cells [147]. Both trimethyl phosphite and trimethyl phosphate reduce the flammability of the electrolyte. The trimethyl phosphite additive is also shown to improve the electrochemical performance whereas trimethyl phosphate improves the thermal stability of the electrolyte at the expense of its electrochemical performance [147].

6 Future Research Challenges and Outlook

This section discusses future research challenges related to experimental investigation of thermal transport in Li-ion cells.

6.1 Thermal Metrology. There is a continued need for improved experimental tools for measuring temperature, heat generation, and thermal transport properties across multiple length scales in Li-ion cells. Measurement of the internal temperature of a cell is a particularly critical challenge for improved performance and safety, since thermal management designs based on surface temperature measurement are likely to be inadequate. Accurate measurement of the internal temperature will also directly benefit electrochemical performance optimization of the cell. Such methods need to be minimally invasive to the electrochemical function of the cell, and be able to monitor the cell temperature in situ while the cell continues to operate. Improvements in sensitivity and response time of temperature measurement methods are needed. Temperature measurement techniques also need to be closely integrated with battery control software.

Metrology tools for material-level temperature measurement are also needed for understanding the fundamentals of thermal transport in electrochemical systems. Such tools need to be closely integrated with electrochemical probing in order to understand and resolve the tradeoffs associated with thermal–electrochemical coupling in materials. Such tools will help resolve the considerable challenges of understanding thermal transport in heterogeneous electrode stacks comprising materials in which the nature of thermal transport through phonons is not well understood at present. Such advances may lead to fundamental, thermal performance-driven improvements in Li-ion materials.

The literature on measurement of thermal transport properties, both at cell-level and at material-level, is quite meager. More work is needed in terms of improved thermal conductivity and heat capacity measurement methods in an electrochemically active environment. There is significant spread in Li-ion cell thermal property measurements reported in various papers so far, and it is important to resolve these differences. At the material level, the metrology and characterization tools are needed for identification of rate-limiting thermal transport processes, with particular emphasis on the nature of thermal transport across material interfaces. The nature of thermal transport in emerging electrochemical materials and cell chemistries needs to be fully understood. Specifically, since a solid electrolyte cell represents a significant departure from the traditional Li-ion cell, it is important to carry out a comprehensive examination of thermal transport in a solid electrolyte cell.

Similar to temperature, noninvasive metrology tools for in situ measurement of heat generation are critical for performance and safety monitoring of Li-ion cells. A method for real-time measurement of heat generation rate will greatly enhance the capability to diagnose and address anomalies in cells and packs. Most heat generation measurement methods so far are calorimetric in nature, which do not integrate well with the operation of the cell. Noncalorimetric tools for heat generation rate measurement, particularly at high discharge rates, are needed.

6.2 Thermal Management. Innovation in thermal management strategies for Li-ion cells is needed to expand the performance limits of a Li-ion cell, which often tends to be thermally limited. At the material level, thermally enhanced materials and interfaces need to be pursued, without affecting the underlying electrochemical performance. Rate-limiting thermal transport processes in materials within a Li-ion cell need to be identified and enhanced for improved overall internal heat transfer in the cell. The thermal conductivity of Li-ion cell is very poor, and strategies for thermal conductivity enhancement are needed.

While several candidate strategies have been presented for external thermal management, more innovation is clearly needed. For example, while water has been used widely for liquid cooling, it suffers from well-known problems that need to be overcome. Smaller heat pipes need to be designed and possibly embedded within a Li-ion cell for efficient heat removal. Hybrid thermal management strategies offer promising results and need to be investigated further. High heat flux cooling methods, including those developed for other applications, need to be studied in the context of cooling Li-ion cells under high discharge rates. Tradeoffs between increased system complexity due to thermal management and benefit on performance and safety need to be characterized. In general, the tradeoff between thermal management and electrochemical performance of cells and battery packs needs to be fully understood and addressed. Integration of thermal management with the battery management system is needed for fully utilizing the benefits of thermal management and for implementing on-demand cooling that offers effective and efficient removal of heat with minimal impact on the electrochemical function of the cell.

6.3 Thermal Runaway. It is expected that much of the future improvement in thermal runaway performance of Li-ion cells will come from innovations in thermal stability of materials and components, and from chemistries with reduced exothermic heat generation at high temperatures. Therefore, innovations in material chemistries are critically needed. Experimentally validated models are also needed to integrate heat generation during runaway conditions with the nature of thermal transport inside the cell and thermal management implemented outside the cell. It is critical to develop analytical tools that can predict the thermal conditions needed to prevent thermal runaway with a given cell chemistry.

Thermal management strategies proposed and demonstrated to work under nominal conditions need to be evaluated on the basis of the ability to suppress thermal runaway under abuse conditions. Future thermal management techniques need to be designed not only for nominal conditions but also for extreme conditions likely to be encountered in a thermal runaway condition, such that they can meet the heat removal demand of an abuse condition.

A reasonable understanding of triggers that cause onset of thermal runaway has been developed. However, there is a lack of understanding of thermal threshold to indicate or anticipate imbalance of heat generated and heat dissipated which could be used to avoid or minimize the risk of thermal runaway. Experimental research in this direction will benefit the design and operation of future energy conversion and storage systems.

Thermal transport phenomena in future electrochemical energy storage chemistries need to be examined for early identification and resolution of key thermal management challenges. Toward this, the thermal transport properties, reaction enthalpies, and heat generation rates in future chemistries need to be measured.

Future research needs in all categories identified above are closely related to each other. Innovations in these directions will benefit multiple aspects of thermal performance of the cell. For example, innovations in internal temperature measurement will positively impact the capability to anticipate and prevent thermal runaway. It is critical to approach these challenges in an integrated fashion that considers each of the thermal transport phenomena discussed here, as well as the close, multiscale coupling of thermal transport with other transport phenomena in a Li-ion cell.

7 Conclusion

The need for continued improvement in performance, safety, and reliability of Li-ion cells makes it imperative to continue to innovate not only in thermal transport phenomena but also in the interactions with other thermal transport processes. The coupled, multiscale nature of physics governing a Li-ion cell makes this a challenging task, with significant potential for performance improvement through fundamental understanding of these processes. These potential improvements may positively impact energy storage and conversion for a wide variety of engineering systems.

Acknowledgment

References

[1] Scrosati, B., and Garche, J., 2010, "Lithium Batteries: Status, Prospects and Future," J. Power Sources, **195**(9), pp. 2419–2430.

[2] Marsh, R. A., Vukson, S., Surampudi, S., Ratnakumar, B. V., Smart, M. C., Manzo, M., and Dalton, P. J., 2001, "Li Ion Batteries for Aerospace Applications," J. Power Sources, **97**, pp. 25–27.

[3] Linden, D., and Reddy, T. B., 2002, *Handbook of Batteries*, 3rd ed., McGraw-Hill, New York.

[4] Khaligh, A., and Li, Z., 2010, "Battery, Ultracapacitor, Fuel Cell, and Hybrid Energy Storage Systems for Electric, Hybrid Electric, Fuel Cell, and Plug-In Hybrid Electric Vehicles: State of the Art," IEEE Trans. Veh. Technol., **59**(6), pp. 2806–2814.

[5] Franco, J. J. L., Boemo, E., Castillo, E., and Parrilla, L., 2010, "Ring Oscillators as Thermal Sensors in FPGAs: Experiments in Low Voltage," VI Southern Programmable Logic Conference (SPL), Ipojuca, Brazil, Mar. 24–26, pp. 133–137.

[6] Diouf, B., and Pode, R., 2015, "Potential of Lithium-Ion Batteries in Renewable Energy," Renewable Energy, **76**, pp. 375–380.

[7] Goodenough, J. B., and Park, K. S., 2013, "The Li-Ion Rechargeable Battery: A Perspective," J. Am. Chem. Soc., **135**(4), pp. 1167–1176.

[8] Wang, C. Y., and Srinivasan, V., 2002, "Computational Battery Dynamics (CBD)—Electrochemical/Thermal Coupled Modeling and Multi-Scale Modeling," J. Power Sources, **110**(2), pp. 364–376.

[9] Sushko, M. L., Rosso, K. M., Zhang, J. G., and Liu, J., 2011, "Multiscale Simulations of Li Ion Conductivity in Solid Electrolyte," J. Phys. Chem. Lett., **2**(18), pp. 2352–2356.

[10] Northrop, P. W., Ramadesigan, V., De, S., and Subramanian, V. R., 2011, "Coordinate Transformation, Orthogonal Collocation, Model Reformulation and Simulation of Electrochemical-Thermal Behavior of Lithium-Ion Battery Stacks," J. Electrochem. Soc., **158**(12), pp. A1461–A1477.

[11] Wang, C. Y., Gu, W. B., and Liaw, B. Y., 1998, "Micro-Macroscopic Coupled Modeling of Batteries and Fuel Cells I. Model Development," J. Electrochem. Soc., **145**(10), pp. 3407–3417.

[12] Ouyang, C., Shi, S., Wang, Z., Huang, X., and Chen, L., 2004, "First-Principles Study of Li Ion Diffusion in LiFePO$_4$," Phys. Rev. B, **69**(10), p. 104303.

[13] Stephan, A. M., and Nahm, K. S., 2006, "Review on Composite Polymer Electrolytes for Lithium Batteries," Polymer, **47**(16), pp. 5952–5964.

[14] Etacheri, V., Marom, R., Elazari, R., Salitra, G., and Aurbach, D., 2011, "Challenges in the Development of Advanced Li-Ion Batteries: A Review," Energy Environ. Sci., **4**(9), pp. 3243–3262.

[15] Zhang, S. S., 2007, "A Review on the Separators of Liquid Electrolyte Li-Ion Batteries," J. Power Sources, **164**(1), pp. 351–364.

[16] Young, K., Wang, C., Wang, L. Y., and Strunz, K., 2013, "Electric Vehicle Battery Technologies," *Electric Vehicle Integration Into Modern Power Networks*, Springer, New York, pp. 15–56.

[17] Bandhauer, T. M., Garimella, S., and Fuller, T. F., 2011, "A Critical Review of Thermal Issues in Lithium-Ion Batteries," J. Electrochem. Soc., **158**(3), pp. R1–R25.

[18] Spotnitz, R., and Franklin, J., 2003, "Abuse Behavior of High-Power, Lithium-Ion Cells," J. Power Sources, **113**(1), pp. 81–100.

[19] Wang, Q., Ping, P., Zhao, X., Chu, G., Sun, J., and Chen, C., 2012, "Thermal Runaway Caused Fire and Explosion of Lithium Ion Battery," J. Power Sources, **208**, pp. 210–224.

[20] Bernardi, D., Pawlikowski, E., and Newman, J., 1985, "A General Energy Balance for Battery Systems," J. Electrochem. Soc., **132**(1), pp. 5–12.

[21] Pals, C. R., and Newman, J., 1995, "Thermal Modeling of the Lithium/Polymer Battery I. Discharge Behavior of a Single Cell," J. Electrochem. Soc., **142**(10), pp. 3274–3281.

[22] Thomas, K. E., and Newman, J., 2003, "Heats of Mixing and of Entropy in Porous Insertion Electrodes," J. Power Sources, **119**, pp. 844–849.

[23] Srinivasan, V., and Wang, C. Y., 2003, "Analysis of Electrochemical and Thermal Behavior of Li-Ion Cells," J. Electrochem. Soc., **150**(1), pp. A98–A106.

[24] Shah, K., Drake, S. J., Wetz, D. A., Ostanek, J. K., Miller, S. P., Heinzel, J. M., and Jain, A., 2014, "Modeling of Steady-State Convective Cooling of Cylindrical Li-Ion Cells," J. Power Sources, **258**, pp. 374–381.

[25] Shah, K., Drake, S. J., Wetz, D. A., Ostanek, J. K., Miller, S. P., Heinzel, J. M., and Jain, A., 2014, "An Experimentally Validated Transient Thermal Model for Cylindrical Li-Ion Cells," J. Power Sources, **271**, pp. 262–268.

[26] Shah, K., and Jain, A., 2015, "Modeling of Steady-State and Transient Thermal Performance of a Li-Ion Cell With an Axial Fluidic Channel for Cooling," Int. J. Energy Res., **39**(4), pp. 573–584.

[27] Zhang, S. S., Xu, K., and Jow, T. R., 2002, "A New Approach Toward Improved Low Temperature Performance of Li-Ion Battery," Electrochem. Commun., **4**(11), pp. 928–932.

[28] Ji, Y., Zhang, Y., and Wang, C. Y., 2013, "Li-Ion Cell Operation at Low Temperatures," J. Electrochem. Soc., **160**(4), pp. A636–A649.

[29] Childs, P. R. N., Greenwood, J. R., and Long, C. A., 2000, "Review of Temperature Measurement," Rev. Sci. Instrum., **71**(8), pp. 2959–2978.

[30] Cooper, T. E., Field, R. J., and Meyer, J. F., 1975, "Liquid Crystal Thermography and Its Application to the Study of Convective Heat Transfer," ASME J. Heat Transfer, **97**(3), pp. 442–450.

[31] Raad, P. E., Komarov, P. L., and Bettiati, M. A., 2014, "Thermoreflectance Temperature Measurements for Optically Emitting Devices," Microelectron. J., **45**(5), pp. 515–520.

[32] Spinner, N. S., Field, C. R., Hammond, M. H., Williams, B. A., Myers, K. M., Lubrano, A. L., Rose-Pehrsson, S. L., and Tuttle, S. G., 2015, "Physical and Chemical Analysis of Lithium-Ion Battery Cell-to-Cell Failure Events Inside Custom Fire Chamber," J. Power Sources, **279**, pp. 713–721.

[33] Koo, B., Goli, P., Sumant, A. V., dos Santos Claro, P. C., Rajh, T., Johnson, C. S., Balandin, A. A., and Shevchenko, E. V., 2014, "Toward Lithium Ion Batteries With Enhanced Thermal Conductivity," ACS Nano, **8**(7), pp. 7202–7207.

[34] Drake, S. J., Martin, M., Wetz, D. A., Ostanek, J. K., Miller, S. P., Heinzel, J. M., and Jain, A., 2015, "Heat Generation Rate Measurement in a Li-Ion Cell at Large C-Rates Through Temperature and Heat Flux Measurements," J. Power Sources, **285**, pp. 266–273.

[35] Lin, X., Perez, H. E., Siegel, J. B., Stefanopoulou, A. G., Li, Y., Anderson, R. D., Ding, Y., and Castanier, M. P., 2013, "Online Parameterization of Lumped Thermal Dynamics in Cylindrical Lithium Ion Batteries for Core Temperature Estimation and Health Monitoring," IEEE Trans. Control Syst. Technol., **21**(5), pp. 1745–1755.

[36] Zhang, G., Cao, L., Ge, S., Wang, C. Y., Shaffer, C. E., and Rahn, C. D., 2014, "In Situ Measurement of Radial Temperature Distributions in Cylindrical Li-Ion Cells," J. Electrochem. Soc., **161**(10), pp. A1499–A1507.

[37] Forgez, C., Do, D. V., Friedrich, G., Morcrette, M., and Delacourt, C., 2010, "Thermal Modeling of a Cylindrical LiFePO$_4$/Graphite Lithium-Ion Battery," J. Power Sources, **195**(9), pp. 2961–2968.

[38] Kim, Y., Mohan, S., Siegel, J. B., Stefanopoulou, A. G., and Ding, Y., 2014, "The Estimation of Temperature Distribution in Cylindrical Battery Cells Under Unknown Cooling Conditions," IEEE Trans. Control Syst. Technol., **22**(6), pp. 2277–2286.

[39] Richardson, R. R., Ireland, P. T., and Howey, D. A., 2014, "Battery Internal Temperature Estimation by Combined Impedance and Surface Temperature Measurement," J. Power Sources, **265**, pp. 254–261.

[40] Li, Z., Zhang, J., Wu, B., Huang, J., Nie, Z., Sun, Y., An, F., and Wu, N., 2013, "Examining Temporal and Spatial Variations of Internal Temperature in Large-Format Laminated Battery With Embedded Thermocouples," J. Power Sources, **241**, pp. 536–553.

[41] Srinivasan, R., Carkhuff, B. G., Butler, M. H., and Baisden, A. C., 2011, "Instantaneous Measurement of the Internal Temperature in Lithium-Ion Rechargeable Cells," Electrochim. Acta, **56**(17), pp. 6198–6204.

[42] Srinivasan, R., Carkhuff, B. G., and Rogers, A. Q., 2012, "Lithium Battery Internal Temperature Sensor and SoC Monitor," The Electrochemical Society (ECS) 18th International Meeting on Lithium Batteries, Chicago, IL, June 19–24, Paper No. 1053.

[43] Srinivasan, R., 2012, "Monitoring Dynamic Thermal Behavior of the Carbon Anode in a Lithium-Ion Cell Using a Four-Probe Technique," J. Power Sources, **198**, pp. 351–358.

[44] Schmidt, J. P., Arnold, S., Loges, A., Werner, D., Wetzel, T., and Ivers-Tiffée, E., 2013, "Measurement of the Internal Cell Temperature Via Impedance: Evaluation and Application of a New Method," J. Power Sources, **243**, pp. 110–117.

[45] Song, L., and Evans, J. W., 1999, "Measurements of the Thermal Conductivity of Lithium Polymer Battery Composite Cathodes," J. Electrochem. Soc., **146**(3), pp. 869–871.

[46] Maleki, H., Al Hallaj, S., Selman, J. R., Dinwiddie, R. B., and Wang, H., 1999, "Thermal Properties of Lithium-Ion Battery and Components," J. Electrochem. Soc., **146**(3), pp. 947–954.

[47] Cho, J., Losego, M. D., Zhang, H. G., Kim, H., Zuo, J., Petrov, I., Cahill, D. G., and Braun, P. V., 2014, "Electrochemically Tunable Thermal Conductivity of Lithium Cobalt Oxide," Nat. Commun., **5**, p. 4035.

[48] Maleki, H., Selman, J. R., Dinwiddie, R. B., and Wang, H., 2001, "High Thermal Conductivity Negative Electrode Material for Lithium-Ion Batteries," J. Power Sources, **94**(1), pp. 26–35.

[49] Goli, P., Legedza, S., Dhar, A., Salgado, R., Renteria, J., and Balandin, A. A., 2014, "Graphene-Enhanced Hybrid Phase Change Materials for Thermal Management of Li-Ion Batteries," J. Power Sources, **248**, pp. 37–43.

[50] Song, L., Chen, Y., and Evans, J. W., 1997, "Measurements of the Thermal Conductivity of Poly(Ethylene Oxide)-Lithium Salt Electrolytes," J. Electrochem. Soc., **144**(11), pp. 3797–3800.

[51] Vishwakarma, V., and Jain, A., 2014, "Measurement of In-Plane Thermal Conductivity and Heat Capacity of Separator in Li-Ion Cells Using a Transient DC Heating Method," J. Power Sources, **272**, pp. 378–385.

[52] Yang, Y., Huang, X., Cao, Z., and Chen, G., 2016, "Thermally Conductive Separator With Hierarchical Nano/Microstructures for Improving Thermal Management of Batteries," Nano Energy, **22**, pp. 301–309.

[53] Maleki, H., Wang, H., Porter, W., and Hallmark, J., 2014, "Li-Ion Polymer Cells Thermal Property Changes as a Function of Cycle-Life," J. Power Sources, **263**, pp. 223–230.

[54] Ponnappan, R., and Ravigururajan, T. S., 2004, "Contact Thermal Resistance of Li-Ion Cell Electrode Stack," J. Power Sources, **129**(1), pp. 7–13.

[55] Vishwakarma, V., Waghela, C., Wei, Z., Prasher, R., Nagpure, S. C., Li, J., Liu, F., Daniel, C., and Jain, A., 2015, "Heat Transfer Enhancement in a Lithium-Ion Cell Through Improved Material-Level Thermal Transport," J. Power Sources, **300**, pp. 123–131.

[56] Zhang, W., Zhang, X., Wang, C., Yu, G., and Yang, C., 2014, "Experimental and Computational Research on the Thermal Conductivities of Li/SOCl$_2$ Batteries," J. Electrochem. Soc., **161**(5), pp. A675–A681.

[57] Drake, S. J., Wetz, D. A., Ostanek, J. K., Miller, S. P., Heinzel, J. M., and Jain, A., 2014, "Measurement of Anisotropic Thermophysical Properties of Cylindrical Li-Ion Cells," J. Power Sources, **252**, pp. 298–304.

[58] Spinner, N. S., Mazurick, R., Brandon, A., Rose-Pehrsson, S. L., and Tuttle, S. G., 2015, "Analytical, Numerical and Experimental Determination of Thermophysical Properties of Commercial 18650 LiCoO₂ Lithium-Ion Battery," J. Electrochem. Soc., **162**(14), pp. A2789–A2795.

[59] Bazinski, S. J., and Wang, X., 2015, "Experimental Study on the Influence of Temperature and State-of-Charge on the Thermophysical Properties of an LFP Pouch Cell," J. Power Sources, **293**, pp. 283–291.

[60] Barsoukov, E., Jang, J. H., and Lee, H., 2002, "Thermal Impedance Spectroscopy for Li-Ion Batteries Using Heat-Pulse Response Analysis," J. Power Sources, **109**(2), pp. 313–320.

[61] Fleckenstein, M., Fischer, S., Bohlen, O., and Bäker, B., 2013, "Thermal Impedance Spectroscopy—A Method for the Thermal Characterization of High Power Battery Cells," J. Power Sources, **223**, pp. 259–267.

[62] Chen, Y., and Evans, J. W., 1994, "Thermal Analysis of Lithium Polymer Electrolyte Batteries by a Two Dimensional Model—Thermal Behaviour and Design Optimization," Electrochim. Acta, **39**(4), pp. 517–526.

[63] Rao, L., and Newman, J., 1997, "Heat-Generation Rate and General Energy Balance for Insertion Battery Systems," J. Electrochem. Soc., **144**(8), pp. 2697–2704.

[64] Chen, Y., and Evans, J. W., 1996, "Thermal Analysis of Lithium-Ion Batteries," J. Electrochem. Soc., **143**(9), pp. 2708–2712.

[65] Hong, J. S., Maleki, H., Al Hallaj, S., Redey, L., and Selman, J. R., 1998, "Electrochemical-Calorimetric Studies of Lithium-Ion Cells," J. Electrochem. Soc., **145**(5), pp. 1489–1501.

[66] Ye, Y., Saw, L. H., Shi, Y., Somasundaram, K., and Tay, A. A., 2014, "Effect of Thermal Contact Resistances on Fast Charging of Large Format Lithium Ion Batteries," Electrochim. Acta, **134**, pp. 327–337.

[67] Al Hallaj, S., Prakash, J., and Selman, J. R., 2000, "Characterization of Commercial Li-Ion Batteries Using Electrochemical–Calorimetric Measurements," J. Power Sources, **87**(1), pp. 186–194.

[68] Zhao, R., Gu, J., and Liu, J., 2014, "An Investigation on the Significance of Reversible Heat to the Thermal Behavior of Lithium Ion Battery Through Simulations," J. Power Sources, **266**, pp. 422–432

[69] Botte, G. G., Subramanian, V. R., and White, R. E., 2000, "Mathematical Modeling of Secondary Lithium Batteries," Electrochimica Acta, **45**(15), pp. 2595–2609.

[70] Chen, K., Unsworth, G., and Li, X., 2014, "Measurements of Heat Generation in Prismatic Li-Ion Batteries," J. Power Sources, **261**, pp. 28–37.

[71] Onda, K., Kameyama, H., Hanamoto, T., and Ito, K., 2003, "Experimental Study on Heat Generation Behavior of Small Lithium-Ion Secondary Batteries," J. Electrochem. Soc., **150**(3), pp. A285–A291.

[72] Kobayashi, Y., Miyashiro, H., Kumai, K., Takei, K., Iwahori, T., and Uchida, I., 2002, "Precise Electrochemical Calorimetry of LiCoO₂/Graphite Lithium-Ion Cell Understanding Thermal Behavior and Estimation of Degradation Mechanism," J. Electrochem. Soc., **149**(8), pp. A978–A982.

[73] Bang, H., Yang, H., Sun, Y. K., and Prakash, J., 2005, "In Situ Studies of Li$_x$Mn₂O₄ and Li$_x$Al$_{0.17}$Mn$_{1.83}$O$_{3.97}$S$_{0.03}$ Cathode by IMC," J. Electrochem. Soc., **152**(2), pp. A421–A428.

[74] Al Hallaj, S., Venkatachalapathy, R., Prakash, J., and Selman, J. R., 2000, "Entropy Changes due to Structural Transformation in the Graphite Anode and Phase Change of the LiCoO₂ Cathode," J. Electrochem. Soc., **147**(7), pp. 2432–2436.

[75] Kim, U. S., Shin, C. B., and Kim, C. S., 2008, "Effect of Electrode Configuration on the Thermal Behavior of a Lithium-Polymer Battery," J. Power Sources, **180**(2), pp. 909–916.

[76] Lu, W., Belharouak, I., Vissers, D., and Amine, K., 2006, "In Situ Thermal Study of Li$_{1+x}$[Ni$_{1/3}$Co$_{1/3}$Mn$_{1/3}$]$_{1-x}$O₂ Using Isothermal Micro-Clorimetric Techniques," J. Electrochem. Soc., **153**(11), pp. A2147–A2151.

[77] Lu, W., and Prakash, J., 2003, "In Situ Measurements of Heat Generation in a Li/Mesocarbon Microbead Half-Cell," J. Electrochem. Soc., **150**(3), pp. A262–A266.

[78] Saito, Y., Kanari, K., and Takano, K., 1997, "Thermal Studies of a Lithium-Ion Battery," J. Power Sources, **68**(2), pp. 451–454.

[79] Yang, H., and Prakash, J., 2004, "Determination of the Reversible and Irreversible Heats of a LiNi$_{0.8}$Co$_{0.15}$Al$_{0.05}$O₂/Natural Graphite Cell Using Electrochemical-Calorimetric Technique," J. Electrochem. Soc., **151**(8), pp. A1222–A1229.

[80] Vaidyanathan, H., Kelly, W. H., and Rao, G., 2001, "Heat Dissipation in a Lithium Ion Cell," J. Power Sources, **93**(1), pp. 112–122.

[81] Kobayashi, Y., Kihira, N., Takei, K., Miyashiro, H., Kumai, K., Terada, N., and Ishikawa, R., 1999, "Electrochemical and Calorimetric Approach to Spinel Lithium Manganese Oxide," J. Power Sources, **81**, pp. 463–466.

[82] Nanda, J., Martha, S. K., Porter, W. D., Wang, H., Dudney, N. J., Radin, M. D., and Siegel, D. J., 2014, "Thermophysical Properties of LiFePO₄ Cathodes With Carbonized Pitch Coatings and Organic Binders: Experiments and First-Principles Modeling," J. Power Sources, **251**, pp. 8–13.

[83] Zhang, S., Zhao, R., Liu, J., and Gu, J., 2014, "Investigation on a Hydrogel Based Passive Thermal Management System for Lithium Ion Batteries," Energy, **68**, pp. 854–861.

[84] Mohammadian, S. K., He, Y. L., and Zhang, Y., 2015, "Internal Cooling of a Lithium-Ion Battery Using Electrolyte as Coolant Through Microchannels Embedded Inside the Electrodes," J. Power Sources, **293**, pp. 458–466.

[85] Park, H., 2013, "A Design of Air Flow Configuration for Cooling Lithium Ion Battery in Hybrid Electric Vehicles," J. Power Sources, **239**, pp. 30–36.

[86] Fathabadi, H., 2014, "A Novel Design Including Cooling Media for Lithium-Ion Batteries Pack Used in Hybrid and Electric Vehicles," J. Power Sources, **245**, pp. 495–500.

[87] Fan, L., Khodadadi, J. M., and Pesaran, A. A., 2013, "A Parametric Study on Thermal Management of an Air-Cooled Lithium-Ion Battery Module for Plug-In Hybrid Electric Vehicles," J. Power Sources, **238**, pp. 301–312.

[88] Yang, N., Zhang, X., Li, G., and Hua, D., 2015, "Assessment of the Forced Air-Cooling Performance for Cylindrical Lithium-Ion Battery Packs: A Comparative Analysis Between Aligned and Staggered Cell Arrangements," Appl. Therm. Eng., **80**, pp. 55–65.

[89] Mahamud, R., and Park, C., 2011, "Reciprocating Air Flow for Li-Ion Battery Thermal Management to Improve Temperature Uniformity," J. Power Sources, **196**(13), pp. 5685–5696.

[90] Wu, M. S., Liu, K. H., Wang, Y. Y., and Wan, C. C., 2002, "Heat Dissipation Design for Lithium-Ion Batteries," J. Power Sources, **109**(1), pp. 160–166.

[91] Giuliano, M. R., Prasad, A. K., and Advani, S. G., 2012, "Experimental Study of an Air-Cooled Thermal Management System for High Capacity Lithium–Titanate Batteries," J. Power Sources, **216**, pp. 345–352.

[92] Xu, X. M., and He, R., 2013, "Research on the Heat Dissipation Performance of Battery Pack Based on Forced Air Cooling," J. Power Sources, **240**, pp. 33–41.

[93] Yu, K., Yang, X., Cheng, Y., and Li, C., 2014, "Thermal Analysis and Two-Directional Air Flow Thermal Management for Lithium-Ion Battery Pack," J. Power Sources, **270**, pp. 193–200.

[94] Wang, T., Tseng, K. J., Zhao, J., and Wei, Z., 2014, "Thermal Investigation of Lithium-Ion Battery Module With Different Cell Arrangement Structures and Forced Air-Cooling Strategies," Appl. Energy, **134**, pp. 229–238.

[95] Jin, L. W., Lee, P. S., Kong, X. X., Fan, Y., and Chou, S. K., 2014, "Ultra-Thin Minichannel LCP for EV Battery Thermal Management," Appl. Energy, **113**, pp. 1786–1794.

[96] Karimi, G., and Dehghan, A. R., 2012, "Thermal Management Analysis of a Lithium-Ion Battery Pack Using Flow Network Approach," Int. J. Mech. Eng. Mechatronics, **1**(1), pp. 88–94.

[97] Tong, W., Somasundaram, K., Birgersson, E., Mujumdar, A. S., and Yap, C., 2015, "Numerical Investigation of Water Cooling for a Lithium-Ion Bipolar Battery Pack," Int. J. Therm. Sci., **94**, pp. 259–269.

[98] Nieto, N., Díaz, L., Gastelurrutia, J., Blanco, F., Ramos, J. C., and Rivas, A., 2014, "Novel Thermal Management System Design Methodology for Power Lithium-Ion Battery," J. Power Sources, **272**, pp. 291–302.

[99] Huo, Y., Rao, Z., Liu, X., and Zhao, J., 2015, "Investigation of Power Battery Thermal Management by Using Mini-Channel Cold Plate," Energy Convers. Manage., **89**, pp. 387–395.

[100] Jarrett, A., and Kim, I. Y., 2011, "Design Optimization of Electric Vehicle Battery Cooling Plates for Thermal Performance," J. Power Sources, **196**(23), pp. 10359–10368.

[101] Jarrett, A., and Kim, I. Y., 2014, "Influence of Operating Conditions on the Optimum Design of Electric Vehicle Battery Cooling Plates," J. Power Sources, **245**, pp. 644–655.

[102] Bandhauer, T. M., and Garimella, S., 2013, "Passive, Internal Thermal Management System for Batteries Using Microscale Liquid–Vapor Phase Change," Appl. Therm. Eng., **61**(2), pp. 756–769.

[103] Hirano, H., Tajima, T., Hasegawa, T., Sekiguchi, T., and Uchino, M., 2014, "Boiling Liquid Battery Cooling for Electric Vehicle," IEEE Transportation Electrification Asia-Pacific Conference (ITEC Asia-Pacific), Beijing, China, Aug. 31–Sept. 3.

[104] van Gils, R. W., Danilov, D., Notten, P. H. L., Speetjens, M. F. M., and Nijmeijer, H., 2014, "Battery Thermal Management by Boiling Heat-Transfer," Energy Convers. Manage., **79**, pp. 9–17.

[105] Yang, X., Yan, Y. Y., and Mullen, D., 2012, "Recent Developments of Lightweight, High Performance Heat Pipes," Appl. Therm. Eng., **33**, pp. 1–14.

[106] Chang, Y. W., Cheng, C. H., Wang, J. C., and Chen, S. L., 2008, "Heat Pipe for Cooling of Electronic Equipment," Energy Convers. Manage., **49**(11), pp. 3398–3404.

[107] Rao, Z., Wang, S., Wu, M., Lin, Z., and Li, F., 2013, "Experimental Investigation on Thermal Management of Electric Vehicle Battery With Heat Pipe," Energy Convers. Manage., **65**, pp. 92–97.

[108] Rao, Z., Huo, Y., and Liu, X., 2014, "Experimental Study of an OHP-Cooled Thermal Management System for Electric Vehicle Power Battery," Exp. Therm. Fluid Sci., **57**, pp. 20–26.

[109] Wang, Q., Jiang, B., Xue, Q. F., Sun, H. L., Li, B., Zou, H. M., and Yan, Y. Y., 2015, "Experimental Investigation on EV Battery Cooling and Heating by Heat Pipes," Appl. Therm. Eng., **88**, pp. 54–60.

[110] Tran, T. H., Harmand, S., and Sahut, B., 2014, "Experimental Investigation on Heat Pipe Cooling for Hybrid Electric Vehicle and Electric Vehicle Lithium-Ion Battery," J. Power Sources, **265**, pp. 262–272.

[111] Tran, T. H., Harmand, S., Desmet, B., and Filangi, S., 2014, "Experimental Investigation on the Feasibility of Heat Pipe Cooling for HEV/EV Lithium-Ion Battery," Appl. Therm. Eng., **63**(2), pp. 551–558.

[112] Zhao, R., Gu, J., and Liu, J., 2015, "An Experimental Study of Heat Pipe Thermal Management System With Wet Cooling Method for Lithium Ion Batteries," J. Power Sources, **273**, pp. 1089–1097.

[113] Burban, G., Ayel, V., Alexandre, A., Lagonotte, P., Bertin, Y., and Romestant, C., 2013, "Experimental Investigation of a Pulsating Heat Pipe for Hybrid Vehicle Applications," Appl. Therm. Eng., **50**(1), pp. 94–103.

[114] Sharma, A., Tyagi, V. V., Chen, C. R., and Buddhi, D., 2009, "Review on Thermal Energy Storage With Phase Change Materials and Applications," Renewable Sustainable Energy Rev., **13**(2), pp. 318–345.

[115] Rao, Z., and Wang, S., 2011, "A Review of Power Battery Thermal Energy Management," Renewable Sustainable Energy Rev., **15**(9), pp. 4554–4571.

[116] Zhou, D., Zhao, C. Y., and Tian, Y., 2012, "Review on Thermal Energy Storage With Phase Change Materials (PCMs) in Building Applications," Appl. Energy, **92**, pp. 593–605.

[117] Waqas, A., and Din, Z. U., 2013, "Phase Change Material (PCM) Storage for Free Cooling of Buildings—A Review," Renewable Sustainable Energy Rev., **18**, pp. 607–625.

[118] Zalba, B., Marín, J. M., Cabeza, L. F., and Mehling, H., 2003, "Review on Thermal Energy Storage With Phase Change: Materials, Heat Transfer Analysis and Applications," Appl. Therm. Eng., **23**(3), pp. 251–283.

[119] Al Hallaj, S., and Selman, J. R., 2000, "A Novel Thermal Management System for Electric Vehicle Batteries Using Phase-Change Material," J. Electrochem. Soc., **147**(9), pp. 3231–3236.

[120] Khateeb, S. A., Farid, M. M., Selman, J. R., and Al-Hallaj, S., 2004, "Design and Simulation of a Lithium-Ion Battery With a Phase Change Material Thermal Management System for an Electric Scooter," J. Power Sources, **128**(2), pp. 292–307.

[121] Khateeb, S. A., Amiruddin, S., Farid, M., Selman, J. R., and Al-Hallaj, S., 2005, "Thermal Management of Li-Ion Battery With Phase Change Material for Electric Scooters: Experimental Validation," J. Power Sources, **142**(1), pp. 345–353.

[122] Mills, A., Farid, M., Selman, J. R., and Al-Hallaj, S., 2006, "Thermal Conductivity Enhancement of Phase Change Materials Using a Graphite Matrix," Appl. Therm. Eng., **26**(14), pp. 1652–1661.

[123] Mills, A., and Al-Hallaj, S., 2005, "Simulation of Passive Thermal Management System for Lithium-Ion Battery Packs," J. Power Sources, **141**(2), pp. 307–315.

[124] Alrashdan, A., Mayyas, A. T., and Al-Hallaj, S., 2010, "Thermo-Mechanical Behaviors of the Expanded Graphite-Phase Change Material Matrix Used for Thermal Management of Li-Ion Battery Packs," J. Mater. Process. Technol., **210**(1), pp. 174–179.

[125] Lin, C., Xu, S., Chang, G., and Liu, J., 2015, "Experiment and Simulation of a LiFePO₄ Battery Pack With a Passive Thermal Management System Using Composite Phase Change Material and Graphite Sheets," J. Power Sources, **275**, pp. 742–749.

[126] Babapoor, A., Azizi, M., and Karimi, G., 2015, "Thermal Management of a Li-Ion Battery Using Carbon Fiber-PCM Composites," Appl. Therm. Eng., **82**, pp. 281–290.

[127] Hémery, C. V., Pra, F., Robin, J. F., and Marty, P., 2014, "Experimental Performances of a Battery Thermal Management System Using a Phase Change Material," J. Power Sources, **270**, pp. 349–358.

[128] Ling, Z., Wang, F., Fang, X., Gao, X., and Zhang, Z., 2015, "A Hybrid Thermal Management System for Lithium Ion Batteries Combining Phase Change Materials With Forced-Air Cooling," Appl. Energy, **148**, pp. 403–409.

[129] Lisbona, D., and Snee, T., 2011, "A Review of Hazards Associated With Primary Lithium and Lithium-Ion Batteries," Process Saf. Environ. Prot., **89**(6), pp. 434–442.

[130] Bro, P., and Levy, S. C., 2013, *Battery Hazards and Accident Prevention*, Springer Science & Business Media, New York.

[131] Park, H. E., Hong, C. H., and Yoon, W. Y., 2008, "The Effect of Internal Resistance on Dendritic Growth on Lithium Metal Electrodes in the Lithium Secondary Batteries," J. Power Sources, **178**(2), pp. 765–768.

[132] Semenov, N. N., 1959, *Some Problems in Chemical Kinetics and Reactivity*, Princeton University Press, Princeton, NJ.

[133] Maleki, H., Deng, G., Anani, A., and Howard, J., 1999, "Thermal Stability Studies of Li-Ion Cells and Components," J. Electrochem. Soc., **146**(9), pp. 3224–3229.

[134] Tobishima, S. I., Takei, K., Sakurai, Y., and Yamaki, J. I., 2000, "Lithium Ion Cell Safety," J. Power Sources, **90**(2), pp. 188–195.

[135] Dahn, J. R., Fuller, E. W., Obrovac, M., and Von Sacken, U., 1994, "Thermal Stability of LiₓCoO₂, LiₓNiO₂ and λ-MnO₂ and Consequences for the Safety of Li-Ion Cells," Solid State Ionics, **69**(3), pp. 265–270.

[136] Belov, D., and Yang, M. H., 2008, "Investigation of the Kinetic Mechanism in Overcharge Process for Li-Ion Battery," Solid State Ionics, **179**(27), pp. 1816–1821.

[137] Feng, X., Fang, M., He, X., Ouyang, M., Lu, L., Wang, H., and Zhang, M., 2014, "Thermal Runaway Features of Large Format Prismatic Lithium Ion Battery Using Extended Volume Accelerating Rate Calorimetry," J. Power Sources, **255**, pp. 294–301.

[138] Yang, H., Bang, H., Amine, K., and Prakash, J., 2005, "Investigations of the Exothermic Reactions of Natural Graphite Anode for Li-Ion Batteries During Thermal Runaway," J. Electrochem. Soc., **152**(1), pp. A73–A79.

[139] Yang, H., Zhuang, G. V., and Ross, P. N., 2006, "Thermal Stability of LiPF₆ Salt and Li-Ion Battery Electrolytes Containing LiPF₆," J. Power Sources, **161**(1), pp. 573–579.

[140] Roth, E. P., and Doughty, D. H., 2004, "Thermal Abuse Performance of High-Power 18650 Li-Ion Cells," J. Power Sources, **128**(2), pp. 308–318.

[141] Sun, Y. K., Myung, S. T., Park, B. C., Prakash, J., Belharouak, I., and Amine, K., 2009, "High-Energy Cathode Material for Long-Life and Safe Lithium Batteries," Nat. Mater., **8**(4), pp. 320–324.

[142] Allcorn, E., and Manthiram, A., 2015, "Thermal Stability of Sb and Cu₂Sb Anodes in Lithium-Ion Batteries," J. Electrochem. Soc., **162**(9), pp. A1778–A1786.

[143] Kim, M., and Park, J. H., 2012, "Inorganic Thin Layer Coated Porous Separator With High Thermal Stability for Safety Reinforced Li-Ion Battery," J. Power Sources, **212**, pp. 22–27.

[144] Cho, T. H., Tanaka, M., Onishi, H., Kondo, Y., Nakamura, T., Yamazaki, H., Tanase, S., and Sakai, T., 2008, "Battery Performances and Thermal Stability of Polyacrylonitrile Nano-Fiber-Based Nonwoven Separators for Li-Ion Battery," J. Power Sources, **181**(1), pp. 155–160.

[145] Zhang, S. S., 2006, "An Unique Lithium Salt for the Improved Electrolyte of Li-Ion Battery," Electrochem. Commun., **8**(9), pp. 1423–1428.

[146] Mandal, B. K., Padhi, A. K., Shi, Z., Chakraborty, S., and Filler, R., 2006, "Thermal Runaway Inhibitors for Lithium Battery Electrolytes," J. Power Sources, **161**(2), pp. 1341–1345.

[147] Yao, X. L., Xie, S., Chen, C. H., Wang, Q. S., Sun, J. H., Li, Y. L., and Lu, S. X., 2005, "Comparative Study of Trimethyl Phosphite and Trimethyl Phosphate as Electrolyte Additives in Lithium Ion Batteries," J. Power Sources, **144**(1), pp. 170–175.

[148] Leising, R. A., Palazzo, M. J., Takeuchi, E. S., and Takeuchi, K. J., 2001, "Abuse Testing of Lithium-Ion Batteries: Characterization of the Overcharge Reaction of LiCoO₂/Graphite Cells," J. Electrochem. Soc., **148**(8), pp. A838–A844.

[149] Maleki, H., and Howard, J. N., 2009, "Internal Short Circuit in Li-Ion Cells," J. Power Sources, **191**(2), pp. 568–574.

[150] Cai, W., Wang, H., Maleki, H., Howard, J., and Lara-Curzio, E., 2011, "Experimental Simulation of Internal Short Circuit in Li-Ion and Li-Ion-Polymer Cells," J. Power Sources, **196**(18), pp. 7779–7783.

[151] Orendorff, C. J., Roth, E. P., and Nagasubramanian, G., 2011, "Experimental Triggers for Internal Short Circuits in Lithium-Ion Cells," J. Power Sources, **196**(15), pp. 6554–6558.

[152] Uchida, I., Ishikawa, H., Mohamedi, M., and Umeda, M., 2003, "AC-Impedance Measurements During Thermal Runaway Process in Several Lithium/Polymer Batteries," J. Power Sources, **119**, pp. 821–825.

[153] Kitoh, K., and Nemoto, H., 1999, "100 Wh Large Size Li-Ion Batteries and Safety Tests," J. Power Sources, **81**, pp. 887–890.

[154] Lopez, C. F., Jeevarajan, J. A., and Mukherjee, P. P., 2015, "Characterization of Lithium-Ion Battery Thermal Abuse Behavior Using Experimental and Computational Analysis," J. Electrochem. Soc., **162**(10), pp. A2163–A2173.

[155] Guo, G., Long, B., Cheng, B., Zhou, S., Xu, P., and Cao, B., 2010, "Three-Dimensional Thermal Finite Element Modeling of Lithium-Ion Battery in Thermal Abuse Application," J. Power Sources, **195**(8), pp. 2393–2398.

[156] Hatchard, T. D., MacNeil, D. D., Basu, A., and Dahn, J. R., 2001, "Thermal Model of Cylindrical and Prismatic Lithium-Ion Cells," J. Electrochem. Soc., **148**(7), pp. A755–A761.

[157] Hatchard, T. D., MacNeil, D. D., Stevens, D. A., Christensen, L., and Dahn, J. R., 2000, "Importance of Heat Transfer by Radiation in Li-Ion Batteries During Thermal Abuse," Electrochem. Solid-State Lett., **3**(7), pp. 305–308.

[158] Lopez, C. F., Jeevarajan, J. A., and Mukherjee, P. P., 2015, "Experimental Analysis of Thermal Runaway and Propagation in Lithium-Ion Battery Modules," J. Electrochem. Soc., **162**(9), pp. A1905–A1915.

[159] Ping, P., Wang, Q., Sun, J., Xiang, H., and Chen, C., 2010, "Thermal Stabilities of Some Lithium Salts and Their Electrolyte Solutions With and Without Contact to a LiFePO₄ Electrode," J. Electrochem. Soc., **157**(11), pp. A1170–A1176.